

# A van der Waals DFT study of chain length dependence of alkanethiol adsorption on Au(111): Physisorption vs. chemisorption

Ersen Mete,<sup>1,\*</sup> Merve Yortanlı,<sup>1</sup> and Mehmet Fatih Danişman<sup>2,†</sup>

<sup>1</sup>*Department of Physics, Balıkesir University, Balıkesir 10145, Turkey*

<sup>2</sup>*Department of Chemistry, Middle East Technical University, Ankara 06800, Turkey*

The energetics and structures of physisorbed and chemisorbed alkanethiols on Au(111) have been systematically investigated up to 10 carbon atoms using van der Waals (vdW) corrected density functional theory (DFT) calculations. The role of chain length, tilting angle and coverage on the adsorption characteristics have been examined to elucidate the energetics and plausible transformation mechanisms between lying down and standing up phases. Coverage and size dependent chain-chain electronic interactions counteract with the alkyl chain-gold surface interactions and the surface relaxation of the metal in the formation of standing up monolayer structures. For the striped phases of long chain alkanethiols, however, our calculations on decanethiol indicates alkyl chain-gold surface interactions to be strong enough to force the molecule to be perfectly parallel to the surface by lifting a gold atom up, in agreement with the proposed models for this film in the literature.

## I. INTRODUCTION

Thiol self-assembled monolayers (SAMs) on Au(111) surfaces continue to attract considerable interest due to their uses in many different applications ranging from organic electronics to biotechnology.<sup>1,2</sup> These systems have been thoroughly investigated both experimentally and theoretically since the pioneering studies in 80's.<sup>3-6</sup> Nevertheless, there are still issues, regarding their fundamental properties, which are not resolved completely.<sup>7-9</sup> To tackle and clarify these issues is not only important from a fundamental surface science point of view but also necessary to improve and control/manipulate the properties of the applications/devices that rely on such SAMs.

The crystal structure of alkanethiol  $[\text{CH}_3(\text{CH}_2)_{n-1}\text{SH}]$ , will be referred to as  $C_n$  SAMs are well established experimentally and it is known that depending on the film density these SAMs have several phases. At low density, the so called striped phases, made up of lying down molecules, form. These have the general structure of  $(p \times \sqrt{3})$  rectangular unit cells where the periodicity,  $p$ , which depends on the film density and the length of the molecule, gives the stripe separation along the gold nearest neighbor direction. Decanethiol is the most studied thiol SAM system and for its lowest density films it has a  $(11 \times \sqrt{3})$  unit cell [some groups report a  $(11.5 \times \sqrt{3})$  unit cell instead] which is also referred to as  $\beta$  phase. Upon increasing coverage a new striped phase forms with a  $(7.5 \times \sqrt{3})$  structure which is also referred to as  $\delta$  phase.<sup>10-15</sup> Hexanethiol, another well studied molecule, on the other hand has a  $(7.5 \times \sqrt{3})$  striped phase.<sup>12,16-18</sup> Similar striped phases were observed for other chain lengths with  $p$  values in accordance with the length of the thiol molecule.<sup>3,4</sup> For the highest density films ( $\theta=1/3$ ) molecules stand up and form the well-known  $(\sqrt{3} \times \sqrt{3})$  R30° unit cell structure with a  $c(4 \times 2)$  superlattice, regardless of the chain length.<sup>3,17,19-21</sup> However, for shorter chain lengths (C1-C3), there are many studies reporting the existence of a  $(3 \times 4)$  structure ei-

ther in coexistence with the  $(\sqrt{3} \times \sqrt{3})$  R30° structure or as the only stable structure which clearly underlines the importance of chain-chain interactions in the film formation mechanism.<sup>22-24</sup> Though, determination of the unit cell structures discussed above were relatively easy through the use of diffraction (X-ray, electron, atom) and scanning probe microscopy (mostly STM) techniques, determination of the exact arrangement of molecules in these unit cells has proved to be a much difficult problem. Hence, a very large number of experimental and theoretical studies have been carried out to clarify this issue most of which were addressing the questions of where the sulfur atom binds on the Au(111) surface and what are the factors that drive the formation of  $c(4 \times 2)$  superlattice.<sup>3,4,8,9,25,26</sup> To this end early computational studies focused on C1 SAMs to determine sulfur binding site since it requires the minimum computational power.<sup>8,25</sup> However, as mentioned above, the chain-chain interactions has a significant effect in the film structure and computational results obtained for C1 SAMs cannot directly be extended to longer chain thiols. Hence in the recent years several density functional theory (DFT) studies (some of which also use van der Waals corrections) have been employed to study longer chain thiol SAMs.<sup>27-35</sup> Nevertheless in almost all of these computational studies the longest thiol studied was C6 and mostly standing up high density films were examined with the aim of determining most favored gold surface reconstruction which seems to be RS-Au<sub>adatom</sub>-SR.

Lying down (striped) phases, though, are particularly important for film formation mechanism, have almost never been studied computationally. Based on gas phase studies it is believed that chemisorption of thiols on Au(111) takes place through a physisorbed precursor state where the thiol molecules are lying down on the surface and relatively mobile.<sup>4,17,25,36</sup> With increasing chain length not only the physisorption energy increases but also the energy barrier between the chemisorbed and physisorbed states  $[(\text{RS-H})_{\text{physAu}} \rightarrow$

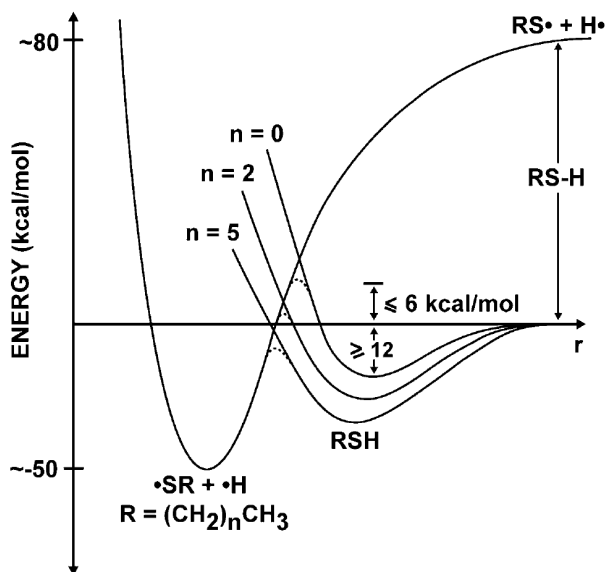


FIG. 1. Reprinted with permission from Ref<sup>17</sup>. Copyright 1993, American Institute of Physics.

RS-Au+1/2H<sub>2</sub>) is suggested to decrease. It was estimated that for chains longer than 6 carbons, energy of the transition state lies below the molecular desorption energy (see Figure 1).<sup>17</sup> In addition, it was found, based on temperature programmed desorption (TPD) measurements, that for chains longer than 14 carbons physisorption energy is higher than the chemisorption energy.<sup>37</sup> Finally, it should be noted that in all the experimental (STM) studies about striped phases the plausibility of the observed unit cell patterns was judged by simply assuming the molecules are perfectly parallel to the gold surface in all-trans fashion or have a tilt angle different than the standing up phases (see for example references [10,11,14,15,38]).

To address these issues and to help interpret the rich experimental findings on striped phases, however, only very few and partial computational studies have been performed.<sup>31,34,35</sup> For instance Ferrighi and coworkers examined low density C4 SAMs in RS-Au<sub>adatom</sub>-SR configuration and found that while with standard DFT (PBE functional) the chemisorption energy does not change with the tilt angle of the molecules, when dispersion corrections were included (M06-L functional) the lying down phase becomes significantly more stable than the standing up phase.<sup>31</sup> Tonigold and Groß performed a similar study for thiols C1 through C6 and found that with PBE functional chemisorption energy does not change significantly (at low density) with changing tilt angle or chain length.<sup>34</sup> However when they used PBD-D3 dispersion correction scheme, though there was no significant change in the chemisorption energy of standing up molecules with changing chain length, for tilted (lying down) molecules it increased significantly with increasing chain length. Finally, Luque and coworkers studied C3

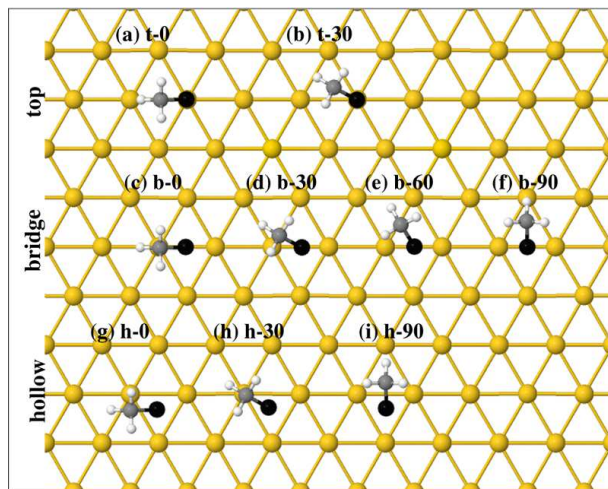


FIG. 2. Possible initial binding geometry models of an isolated alkanethiol on Au(111) surface. For visual convenience methanethiol (C1) is depicted as a representative. The labeling starts with the first letter of chemisorption site of sulphur atom (in black), then the angle (in degrees) between the major axis of the molecule and the gold row follows after that.

SAMs and compared the physisorbed and chemisorbed states of standing up and lying down phases at different coverages and for different Au surface reconstructions/defects (e.g. adatom, vacancy).<sup>35</sup> Though they considered the van der Waals interactions only through the use of a simple universal force field approach, interestingly they found for a defect free surface chemisorption energy of a standing up molecule to be higher than that of lying down molecule regardless of the coverage. On the other hand, for sulfur binding to an Au adatom or on top of an Au vacancy site chemisorption strength was strongly depending on the coverage and for certain coverage values lying down phases had higher chemisorption energy.

To address the issues summarized above regarding striped phases of thiol SAMs here we present a systematic vdW-DFT study of physisorption and chemisorption of thiols C1 through C10. First we discuss the physisorption of isolated lying down thiols on defect free (unreconstructed) Au(111) surface. Then we present the chemisorption energies for the same configurations and compare these energies as a function of chain length in order elucidate physisorption to chemisorption transition mechanism/energetics. Finally, we study the adsorption energies for full monolayer C10 films in lying down ( $11 \times \sqrt{3}$ ) and C1, C3, C4, C6, C8, and C10 films in standing up [ $(\sqrt{3} \times \sqrt{3})R30^\circ$ ] configurations with the aim of elaborating on the experimentally determined striped phase unit cell structures.

## II. THEORETICAL METHODS

The minimum energy geometries of alkanethiols on the (111) surface of gold have been determined based on density functional theory (DFT) calculations using VASP.<sup>39,40</sup> Electron-ion interactions were included within the framework of the projector-augmented wave (PAW)<sup>41,42</sup> method using the plane wave expansion for the single particle states up to a cutoff value of 400 eV.

For weakly interacting organic-organic and metal-organic systems, van der Waals forces need to be included in the calculations. Extensive tests have been made to get a proper description of the dispersive forces. Meanwhile, the lattice structure of metals, in which van der Waals interactions are negligibly small, should not be distorted. For instance, the experimental lattice constant of bulk gold is 4.078 Å.<sup>43</sup> The vdW-DF2<sup>44</sup> functional gives a value of 4.33 Å while it turns out as 4.16 Å with the standard PBE functional. The density dependent dispersion correction (dDsC)<sup>45,46</sup> scheme leads to a lattice parameter of 4.11 Å for gold. The dDsC approach not only is computationally efficient but also yields reasonably accurate results among the other functionals for gold-alkanethiol structures tested here. These findings are in agreement with a recent benchmarking study of a similar platinum-molecular system.<sup>47</sup>

In order to consider isolated molecules (C1–C10) on Au(111), a number of  $p(n \times m)$  slab models with various surface periodicities have been constructed, where  $n, m$  are suitably chosen integers. For instance, a single C1 can be thought isolated on a  $p(4 \times 4)$  slab. Similarly, a  $p(7 \times 5)$  cell provides enough room for a C10 molecule to be separated from its periodic images. A  $(\sqrt{3} \times \sqrt{3})R30^\circ$  and a  $(11 \times \sqrt{3})$  supercell structure has been formed to simulate C1, C3, C4, C6, C8, C10 standing up and C10 lying down full monolayer phases, respectively. These supercell models are chosen in accordance with the experimentally assigned surface structures.<sup>4,9,11,22</sup> All computational cells consist of a slab with four layers of gold, molecular adsorbates and a vacuum region of at least 12 Å thick. Brillouin zone integrations were performed with Methfessel-Paxton smearing of 0.1 over appropriate  $\mathbf{k}$ -point grids which both obey the translational symmetry of the corresponding supercell and yield a  $10^{-4}$  eV convergence in the total energies. For instance,  $6 \times 6 \times 1$  and  $3 \times 5 \times 1$   $\Gamma$ -centered  $\mathbf{k}$ -meshes were used for  $p(4 \times 4)$  and  $p(7 \times 5)$  real space structures. The geometry optimizations were performed self-consistently both with and without the vdW corrections by requiring the Hellmann-Feynman forces on each ion in each direction to be less than  $10^{-2}$  eV·Å<sup>-1</sup>. We used the corresponding lattice constant of gold obtained for each type of exchange-correlation functional in the slab calculations. After achieving a full relaxation of the clean surface models, the ionic positions in the bottom layer were kept frozen in subsequent molecular adsorption calculations.

The adsorption energy per alkanethiol molecule on

Au(111) surface can be calculated using,

$$E_a = (E_{Cn+Au(111)} - E_{Au(111)} - mE_{Cn})/m,$$

where  $E_{Cn+Au(111)}$  is the total supercell energy of Au(111) slab with  $m$  number of  $Cn$  molecules,  $E_{Au(111)}$  and  $E_{Cn}$  are the energies of the bare Au(111) slab and of a single  $Cn$  in the gas phase, respectively. In chemisorption cases,  $Cn$  refers to the molecule where the hydrogen atom is removed from the thiol group. Adsorption energies,  $E_a$ , will be referred to as  $E_p$  for physisorption and  $E_c$  for chemisorption, in addition “dDsC” and “PBE” will be used as subscripts to distinguish the adsorption energies calculated by these methods when necessary. Finally, we should remark that when adsorption energies are compared in the discussion part, always the magnitudes (absolute values) will be considered.

## III. RESULTS AND DISCUSSION

### Isolated Alkanethiols on Au(111)

Single isolated alkanethiols were considered with all probable initial configurations for physisorption and chemisorption on Au(111) surface. The symmetrically distinct structures are shown in Figure 2 where the C1 is chosen as a representative for visual convenience. The  $3p^4$  valance property allows sulphur atom to interact with gold more strongly relative to the atoms at the carbon chain. Hence, hydrogen deficient thiol drives the molecules to the bridge site in all of the geometry optimization calculations starting with any of the initial chemisorption configurations given in Figure 2. As a result, the alkanethiols energetically prefer the b-90 position with the formation of two S-Au bonds as shown in Figure 3. Inclusion of the vdW corrections has a little effect on the binding site and brings slight differences in the structural parameters like bond lengths and tilting angles (in Table I) of isolated molecules on gold. Since for longer chains there is significant bending in the molecule, the tilting angle is calculated by using the line connecting sulfur atom to the last carbon on the chain. In particular, the PBE S-Au bond lengths increase from around 2.46 Å for C1 to 2.48 Å for C10 while the PBE+dDsC ones are less dependent on the chain size giving a value of 2.48 Å on the average. However, the values obtained with these two different functionals converge to each other as the chain lengths increase. On the other hand, the tilting of the molecules with respect to the gold (111) plane seems to be noticeably smaller with the vdW corrections. Moreover, the difference in the tilting angles gets bigger for C4–C7 for which long-ranged dispersive forces between the surface and the carbon chain becomes important for these midsize molecules. Apparently, the height of the tips of the chemisorbed alkanethiols from the surface is always larger with the PBE functional. This is not surprising

TABLE I. The average S-Au bond lengths ( $d_{S-Au}$  in angstroms), the tilting angles ( $\theta$  in degrees) and the heights of the carbon atoms at the tip ( $h_{tip}$  in angstroms) of isolated alkanethiol molecules on Au(111) using both PBE and PBE+dDsC functionals.

	Physisorption						Chemisorption					
	PBE			PBE+dDsC			PBE			PBE+dDsC		
	$d_{S-Au}$	$\theta$	$h_{tip}$	$d_{S-Au}$	$\theta$	$h_{tip}$	$d_{S-Au}$	$\theta$	$h_{tip}$	$d_{S-Au}$	$\theta$	$h_{tip}$
methane	2.66	25.8	4.46	2.62	22.8	4.33	2.46/2.47	34.1	3.92	2.47/2.48	33.9	3.74
ethane	2.66	21.3	4.44	2.62	20.1	4.31	2.47/2.47	36.0	4.54	2.48/2.48	33.8	4.15
propane	2.67	19.8	5.06	2.62	17.7	4.78	2.46/2.47	35.4	5.41	2.48/2.49	31.7	4.97
butane	2.67	16.7	5.10	2.62	14.5	4.70	2.46/2.47	32.2	5.57	2.48/2.49	23.0	4.84
pentane	2.66	11.8	5.08	2.63	10.4	4.78	2.46/2.47	30.5	6.41	2.49/2.49	18.7	5.04
hexane	2.67	11.9	5.19	2.63	8.4	4.66	2.46/2.47	24.9	6.02	2.47/2.48	13.6	4.77
heptane	2.70	8.8	5.15	2.66	6.8	4.63	2.47/2.48	16.2	5.57	2.48/2.49	10.5	4.65
octane	2.69	6.8	4.98	2.64	5.2	4.61	2.48/2.49	13.3	5.38	2.48/2.49	9.4	4.62
nonane	2.69	5.7	5.01	2.64	4.4	4.59	2.48/2.49	11.1	5.28	2.48/2.49	8.2	4.69
decane	2.67	5.2	4.87	2.64	4.1	4.58	2.48/2.48	8.7	4.98	2.48/2.48	6.7	4.49

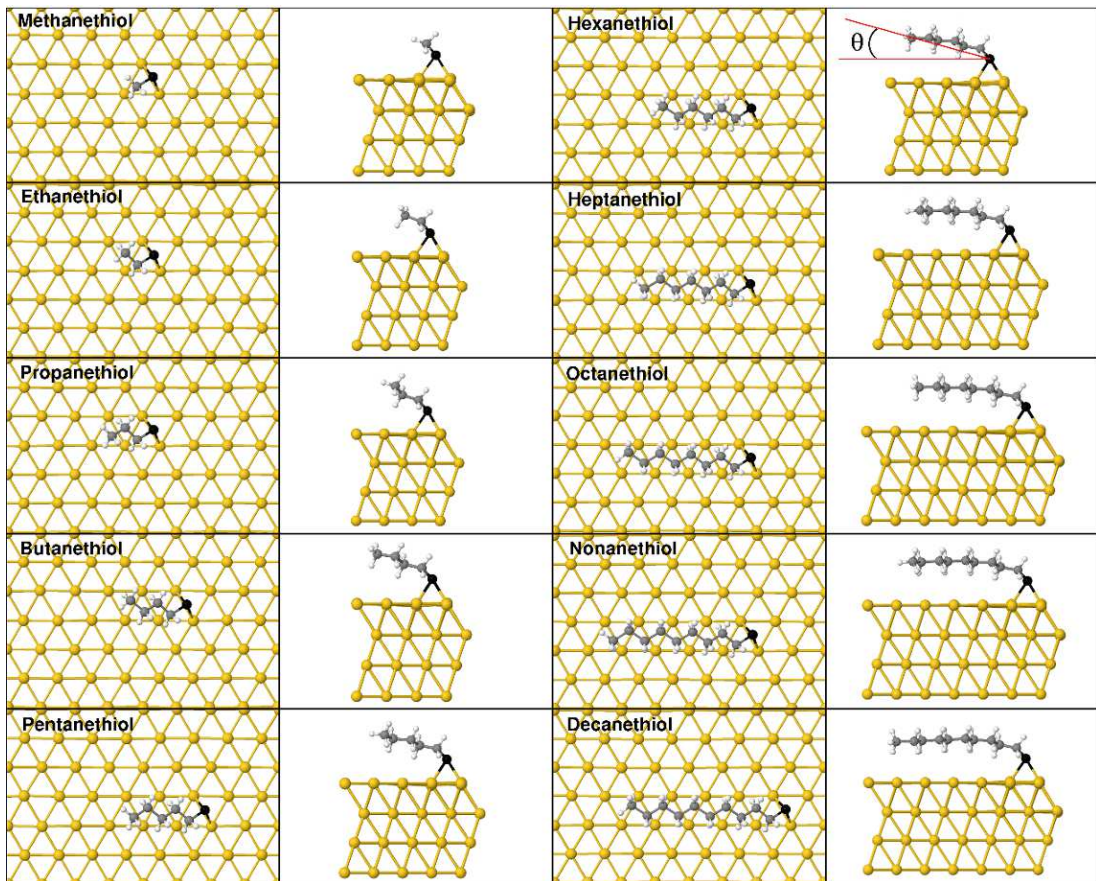


FIG. 3. Chemisorption geometries of isolated alkanethiols on Au(111) surface optimized using the PBE+dDsC vdW corrected DFT calculations. The top and side views are presented for C1 up to C10 molecule. The tilting angle,  $\theta$ , is measured between the surface parallel and the line connecting the sulphur atom to the last carbon at the tip of the corresponding molecule.

since vdW functional is expected to account for dispersion interaction better than PBE which in turn results in approaching of the chain tip to the surface, especially so for the longer chains that have larger flexibility.

Geometry optimizations were also carried out for the physisorption of alkanethiols (in Figure 4). As a trend, the thiol part energetically relax in the top site with the alkyl groups lying in between two adjacent gold rows where carbon atoms are attracted to the nearest surface gold atoms. The physisorbed molecules always end up with significantly smaller tilting angles relative to their chemisorbed counterparts. As expected, the tilting exhibits an inverse proportionality with the chain length. In addition, considerable bending starting from the S-C bond toward the tip results due to the S-Au interaction which especially leads to a bond formation in the chemisorption of C7-C10. Molecular bending through the major axis is relatively less in the physisorption cases where the S-Au distance is significantly larger. PBE functional gives values between 2.66 Å and 2.70 Å for the S-Au distance while the vdW corrections yield values between 2.62 Å and 2.66 Å.

The calculated physisorption and chemisorption energies are reported in Table II. PBE physisorption energies ( $E_{p,PBE}$ ) indicate a weak interaction of the thiol compounds with the gold surface. On the other hand, dDsC physisorption energies ( $E_{p,dDsC}$ ) are larger and increase significantly with increasing chain length due to the long range correlation effects between the non-overlapping charge densities. These effects are clearly visible in the plots provided in Figure 5 which show the adsorption energies as a function of chain length. In case of the PBE functional, physisorption energy increases linearly with chain length but with a slope of only -0.011 eV/n, on the other hand with the dDsC functional the slope is one order of magnitude larger (-0.12 eV/n). One interesting point to note here is that with PBE functional C10 physisorption energy does not follow this trend and is higher than what the linear fit predicts. When the geometry of physisorbed C10 is compared with the other physisorbed thiols (C1-C9) no significant difference can be observed which makes it difficult to predict the reason of this deviation in the physisorption energy of C10.

When the chemisorption energies with and without dispersion corrections are compared, a trend similar to what is discussed above for physisorption can be observed. The chemisorption energy with the PBE functional, ( $E_{c,PBE}$ ), is almost constant (at about -1.9 eV). If a linear fit is forced however, a decrease with increasing chain length can be found with a slope of 0.011 eV/n (with a poor  $R^2$  value of 0.68). Very interestingly C10 chemisorption energy does not follow this trend and is significantly higher (in magnitude) than what the linear fit predicts. Since this was also the case in the physisorption, the nature of the cause of this deviation (in the PBE binding energies of C10) may be the same for both physisorption and chemisorption. When the dDsC chemisorption energies are examined ( $E_{c,dDsC}$ ), a signif-

TABLE II. Adsorption energies (eV) of isolated alkanethiol molecules on Au(111) calculated using both PBE and PBE+dDsC functionals.

	Physisorption		Chemisorption	
	PBE	PBE+dDsC	PBE	PBE+dDsC
methane	-0.35	-1.01	-1.88	-2.54
ethane	-0.36	-1.13	-1.89	-2.67
propane	-0.38	-1.20	-1.90	-2.75
butane	-0.39	-1.28	-1.90	-2.83
pentane	-0.40	-1.36	-1.87	-2.92
hexane	-0.41	-1.50	-1.86	-2.98
heptane	-0.41	-1.64	-1.81	-3.05
octane	-0.42	-1.82	-1.82	-3.22
nonane	-0.45	-1.93	-1.81	-3.34
decane	-0.60	-2.13	-1.98	-3.56

icant increase (in magnitude) can be observed with increasing chain length. This change is pretty linear with a slope of -0.10 eV/n. It is not surprising that the slopes of chemisorption and physisorption plots with PBE+dDsC (will be referred to as  $S_c$  and  $S_p$  respectively) are similar, since in the chemisorption case the Au-S binding energy is more or less independent of the chain length (as evidenced by PBE chemisorption energy values) whereas the alkyl chain-gold surface interaction increases almost to the same extent it increases in the physisorption.

Experimentally, physisorption of alkane thiols as a function of chain length was studied by Scoles group and the desorption energy was found to increase with a slope of 0.063 eV/n.<sup>37</sup> This value is about the half of what we found here either for chemisorption or physisorption. One reason may be the fact that the results we obtained are for isolated molecules whereas the experimental values were obtained by desorbing a full monolayer of physisorbed film. In general, however, computational studies find the binding energies of isolated molecules to be larger (in magnitude) than the binding energies for a monolayer.<sup>35,48-50</sup> In fact, this is the case in this study as well and, as will be discussed in the next section, we found the binding energies of a full monolayer of C10 (either physisorbed or chemisorbed) to be lower than that of isolated C10 molecules.

The difference between the chemisorption and physisorption energies as a function of chain length is another parameter than can be considered for comparing the strength of hydrocarbon chain-gold and sulfur-gold interactions. In Figure 6a the magnitude of this difference ( $E_c - E_p$ ) is plotted for both PBE and PBE+dDsC adsorption energies. As can be seen, with PBE, the difference decreases (in magnitude) gradually from C1 to C10. However, the rate of this decrease is largest in the range of C4 to C7. In case of PBE+dDsC adsorption energies, on the other hand, there is no such trend. In fact, the difference first increases (in magnitude) slowly up to C5 and then suddenly decreases and stays almost



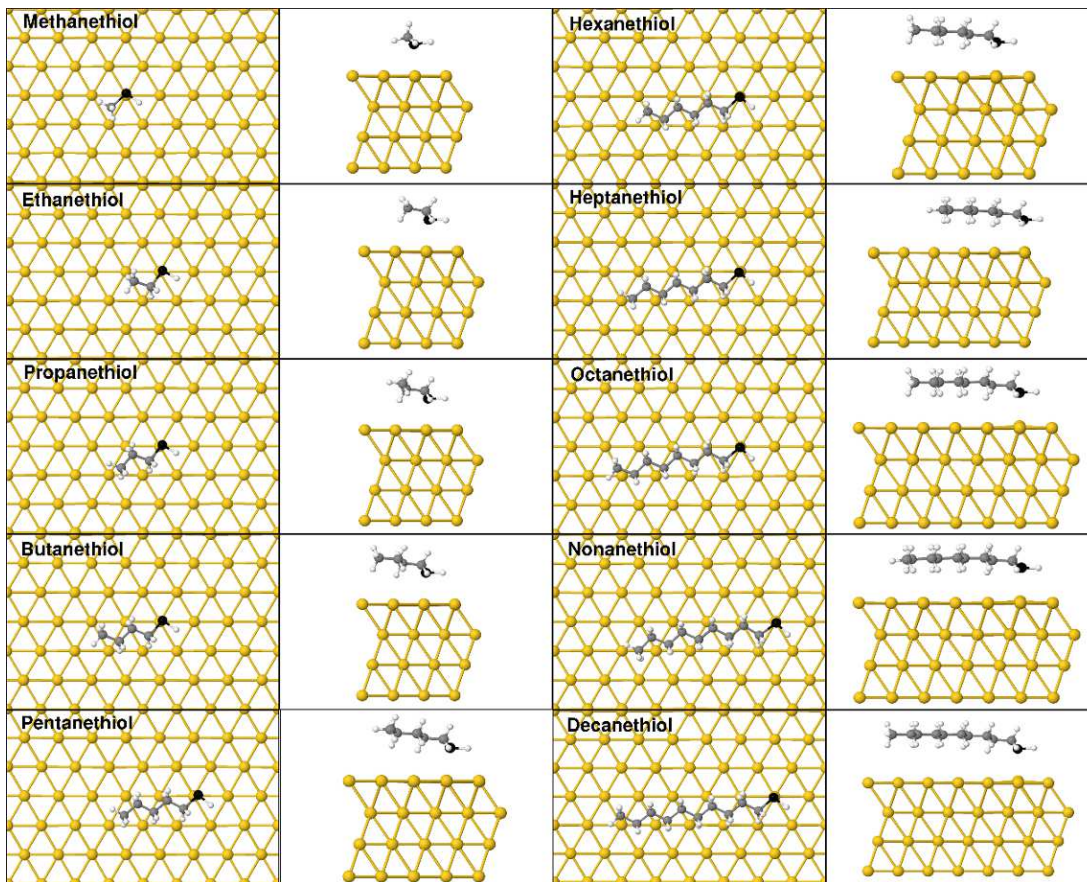


FIG. 4. Physisorption geometries of isolated alkanethiols on Au(111) surface optimized using the PBE+dDsC vdW corrected DFT calculations. The top and side views are presented for C1 up to C10 molecule.

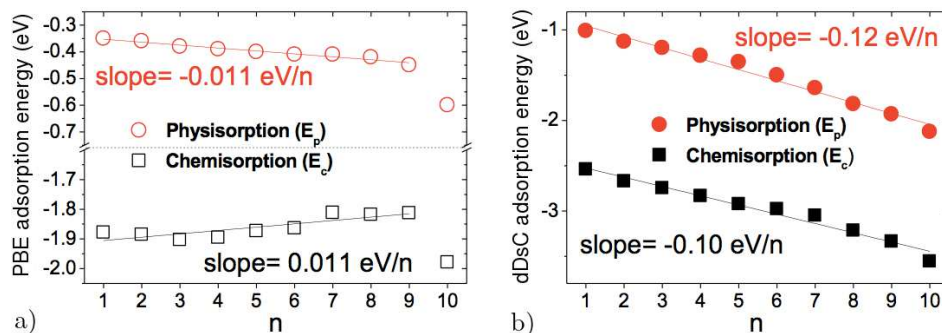


FIG. 5. Calculated physisorption and chemisorption energy plots of isolated alkanethiols on Au(111) with PBE and PBE+dDsC functionals.

constant. This behavior is in fact strongly correlated to the tilt angle difference between the physisorbed and chemisorbed molecules ( $\theta_c - \theta_p$ ) as shown in Figure 6b. As the length of the molecule increases, it becomes more flexible and the tilt angle of the chemisorbed state (which is constrained for short chains by the Au-S bond) approaches to that of the physisorbed state. This transition takes place at chain length of 5-6 carbon atoms as clearly visible in the plots.

### Alkanethiol Monolayers on Au(111)

In order to compare the binding characteristics of the alkanethiols in full monolayers with their isolated phases on gold, we modeled the experimentally observed  $(\sqrt{3} \times \sqrt{3})R30^\circ$  surface cell for C1, C3, C4, C6, C8 and C10. As discussed in the introduction section, for full monolayers of standing up thiols, the existence of  $(\sqrt{3} \times \sqrt{3})R30^\circ$  structure has been shown by many experimental studies. There are many discussions regard-

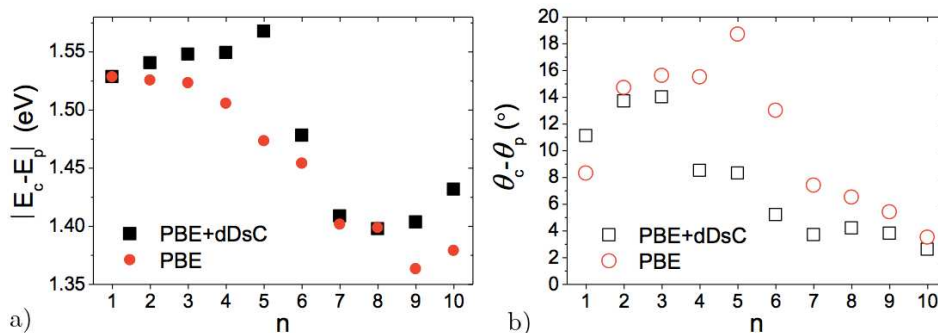


FIG. 6. Energy and tilting angle differences between chemisorbed and physisorbed isolated alkanethiols using PBE and PBE+dDsC functionals.

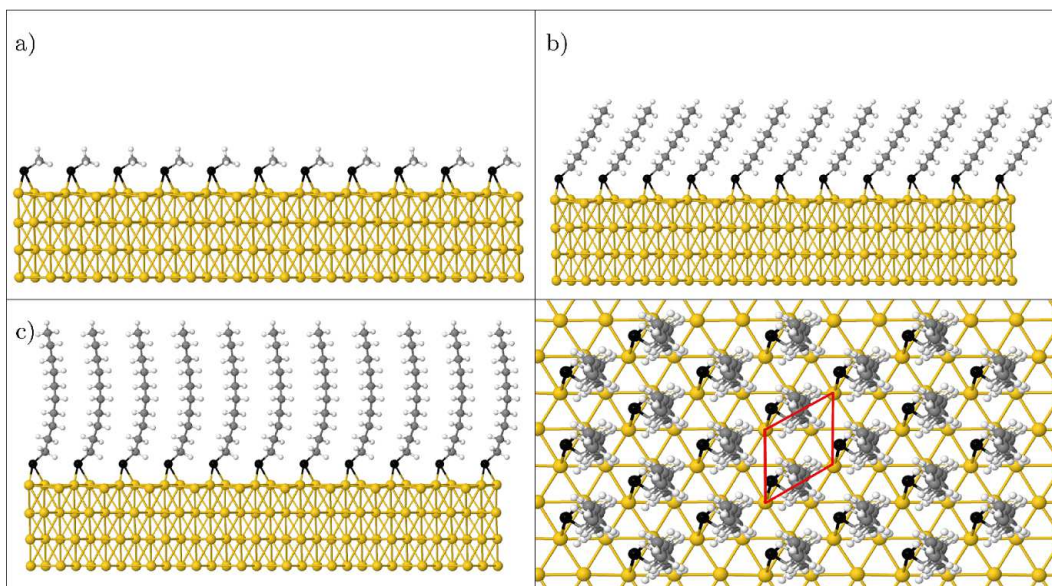


FIG. 7. One full monolayer of a) C1, b) C6, and c) C10 on Au(111) with  $(\sqrt{3} \times \sqrt{3})R30^\circ$  optimized with PBE+dDsC vdW corrected DFT functional. Surface unit cell is indicated in the bottom right panel (top view of C10 SAM).

ing the nature of this unit cell, such as adsorption site of the sulphur atoms, gold surface reconstructions and chain-chain interactions. Here our aim is not to address all of these issues. Instead we want to focus on the chain-chain interactions on an unreconstructed surface and discuss/compare the chain length dependence of adsorption energies for isolated and full monolayer thiols. Probable initial configurations were taken into account including top, bridge, and hollow sites and optimized using the vdW corrected PBE+dDsC functional (in Figure 7). As the chain length increases tilt angle of the molecules increases gradually from  $29^\circ$  for C1 up to  $80^\circ$  for C10 SAMs. More interestingly, the thiolates start to bend as the carbon chain length increases. In particular, C10 exhibits a significant molecular bending at its  $(\sqrt{3} \times \sqrt{3})R30^\circ$  SAM structure as shown in Figure 7c. The binding sites and the Au-S bonds are not affected from the molecular size as given in Table III. On the other hand, the S-C bond angle with respect to the sur-

face plane increases from  $29.1^\circ$  for C1 to  $37.2^\circ$  for C3 and stays approximately constant up to C10. Moreover, longer molecules are bent more between their thiol group and alkyl chains. This can be explained by the existence of two different interaction strengths. The thiol-gold interaction is much stronger in comparison with the long-ranged intermolecular interactions which are essentially between the alkyl parts of neighboring molecules. The anchoring structure of the thiol part rather seems to be less affected by the carbon chain length. As a result, weaker intermolecular interactions signify the important role of the alkyl size on the final geometries. From a theoretical point of view, that necessitates the use of vdW corrected functionals in the DFT calculations (Table IV).

The PBE+dDsC calculations show that the binding energy per molecule in a full monolayer ( $E_{ML}$ ) increases with the increasing length of the carbon chain as plotted in Figure 8a comparatively with the binding energies of isolated molecules ( $E_I$ ). In fact, the chain length de-



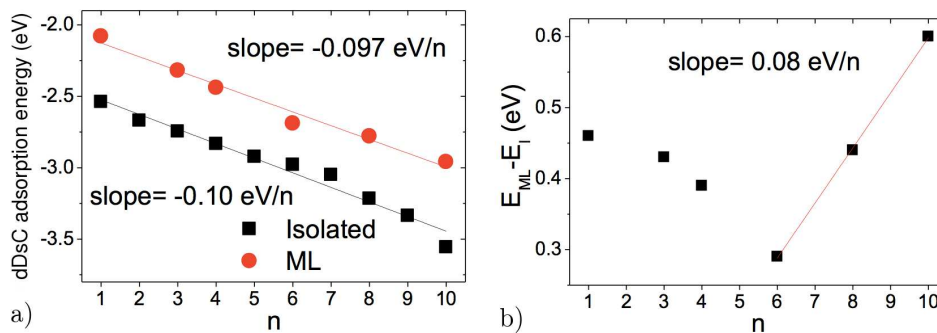


FIG. 8. Chemisorption energy plots of isolated and full monolayer  $[(\sqrt{3} \times \sqrt{3})R30^\circ]$  alkanethiols on Au(111) optimized with vdW corrected DFT calculations.

TABLE III. Bond lengths ( $\text{\AA}$ ), tilting angles (in degrees) and average binding energies per molecule (eV) of various alkanethiols at full monolayer coverage on gold, calculated using the PBE+dDsC method.

Au(111)- $(\sqrt{3} \times \sqrt{3})R30^\circ$					
	$d_{S-Au}$	$d_{S-C}$	$\theta_{S-C}$	$\theta$	$E_a$
methane	2.50/2.51	1.82	29.1	29.1	-2.08
propane	2.49/2.49	1.83	37.2	49.8	-2.32
butane	2.48/2.49	1.82	37.6	52.9	-2.44
hexane	2.48/2.49	1.82	37.6	56.3	-2.69
octane	2.47/2.50	1.83	37.8	69.4	-2.78
decane	2.48/2.50	1.83	37.7	82.5	-2.96

TABLE IV. Average adsorption energies per decanethiol (eV) in the striped phase at full monolayer coverage on gold, calculated using the PBE+dDsC method.

Decanethiol/Au(111)- $(11 \times \sqrt{3})$			
striped phase	$E_a$	$d_{S-Au}$	$h_{tip}$
physisorption	-1.32	3.89/2.68	4.56/4.56
chemisorption	-3.03	2.43/2.57	4.56/4.56

pendence of  $E_{ML}$  is pretty linear and have a slope of  $-0.097 \text{ eV/n}$  (with  $R^2$  of 0.97). This is expected since, as the molecule length increases the vdW interactions between the chains get stronger. Interestingly, however, the slope for standing up monolayer, is almost equal to the slope for lying down isolated molecules. Increasing binding strength with chain length was also observed by Salvarezza group who studied monolayers of C1, C4 and C6 by using optB88-vdW functional to account for the vdW interactions.<sup>28</sup> However, another probable contribution to this increase in the binding energies can be that, for longer chain thiolates, there are relatively more unoccupied molecular energy levels available near the Fermi energy of the metal surface to allow a larger amount of charge transfer from the 11  $d$ -states of gold to the empty frontier molecular levels.

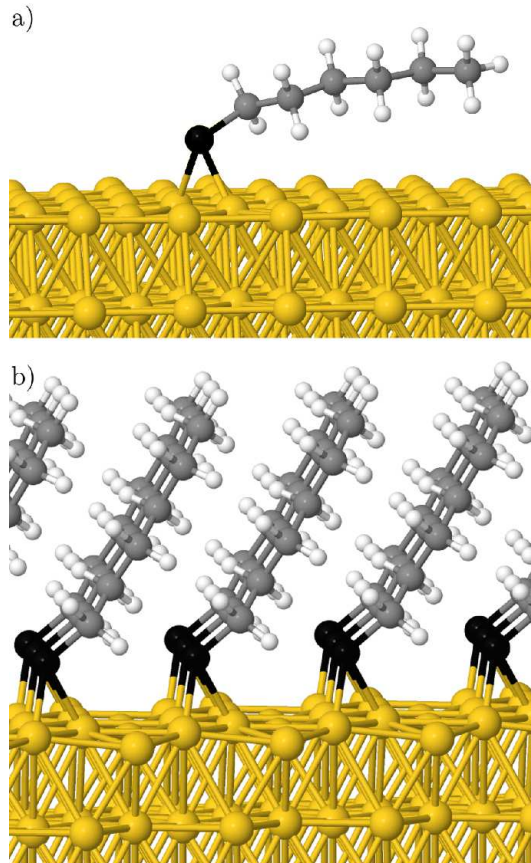


FIG. 9. Comparison of surface structures of a) isolated and b) full monolayer hexanethiol on Au(111) optimized with vdW corrected DFT calculations.

To have a better interpretation of this chain length dependence of  $E_{ML}$ , binding energies of the isolated molecules,  $E_I$ , can be compared with  $E_{ML}$ . As can be seen in Figure 8b,  $E_I$  is always larger (in magnitude) than the corresponding  $E_{ML}$ , however their difference ( $E_{ML} - E_I$ ) does not have a linear dependence on the chain length. Decreasing of the adsorption energy of thiols with increasing coverage was also observed in several other



computational studies<sup>35,48–50</sup> and this is generally attributed to the gold surface reconstructions/relaxations becoming more difficult at higher coverages. Our results indicate a similar mechanism: Each sulphur atom at the bridge site pulls two adjacent gold atoms by  $\sim 0.3$  Å up from the (111) plane. Especially, at the full monolayer coverage, closely packed alkanethiols put an additional stress on the gold surface. As a result, the remaining gold atoms on the upper plane, which are not coordinated with any sulphur, are forced to sink a little down leading to a corrugated surface look (e.g. as recognized from Figure 9 for C6 in its isolated and SAM phases). Therefore, surface relaxation becomes more difficult relative to isolated cases. With these in mind, the chain length dependence of  $(E_{\text{ML}} - E_{\text{I}})$  can be explained as follows: In the isolated case, for C1 to C6, the molecules have high tilt angle and hence low alkyl chain-gold surface interaction. As a result, in the ML case these molecules do not lose much stabilization due to the absence of alkyl chain-gold surface interaction (in the ML). In fact, the stabilization due to chain-chain interactions present in the ML case can more than compensate the lost alkyl chain-gold surface interaction (present in the isolated case). However, this (chain-chain interactions) is still not strong enough to compensate for the destabilization due to gold surface stress in the ML. Hence,  $(E_{\text{ML}} - E_{\text{I}})$  though always positive, decreases from C1 to C6, since increasing chain length means stronger chain-chain interactions in the ML. For alkane chains longer than 6 carbons, however, in the isolated case there is significant alkyl chain-gold surface interaction strength and the chain-chain interactions in the ML is not strong enough to compensate the lost alkyl chain-gold surface interactions. Hence,  $(E_{\text{ML}} - E_{\text{I}})$  starts to increase after C6 perfectly linearly with a slope of 0.08 eV/n and gets its largest value for C10.

To be able to compare physisorption and chemisorption also for full monolayer coverage films and to provide theoretical insight to the striped phase unit cell models reported in the literature we investigated the Au(111)- $(11 \times \sqrt{3})$  structure of decanethiol as well by PBE+dDsC calculations. The optimized geometries for both physisorption and chemisorption are shown in Figure 10. In the chemisorption case, the sulphur atoms lift the surface gold atom up by 0.65 Å, whereas in the physisorption case, one of the sulphur atoms approaches the surface significantly, in order for the molecules to fit in the unit cell. Other than these differences the arrangement of the carbon chain in the unit cell is identical in both cases. Our results indicate that  $(11 \times \sqrt{3})$  unit cell models reported in the literature (with flat lying down C10 molecules) were in fact pretty accurate even though they were not based on any computational study. One interesting point to note here is that even though we have not considered reconstructed gold surfaces in here (like gold adatoms as discussed in the introduction), the interaction of the long C10 chain with the gold surface is strong enough to force the molecule to an almost perfectly flat configuration by lifting one gold atom from the surface in the

chemisorption case. Hence (though not an adatom) a reconstruction similar to RS-Au<sub>adatom</sub>-SR model reported in the literature<sup>22,51</sup> takes place on the surface.

When the energetics of structures is considered, it can be seen that chemisorbed monolayer is much more stable than the physisorbed one, as expected. As in the case of  $(\sqrt{3} \times \sqrt{3})$  monolayer, the chemisorption energy of  $(11 \times \sqrt{3})$  structure ( $E_{c,(11 \times \sqrt{3})} = -3.03$  eV) is lower (in magnitude) than that of the isolated C10 ( $E_{c,C10} = -3.56$  eV). This decrease is most probably due to the energy spent on lifting one gold atom (per unit cell) from the surface. Interestingly, however, the binding energy of the physisorbed  $(11 \times \sqrt{3})$  monolayer ( $E_{p,(11 \times \sqrt{3})} = -1.32$  eV) is also lower (in magnitude) than that of the physisorbed isolated C10 (-3.03 eV). The difference in this latter case is much larger and is probably due to the short S-Au distance of one of the molecules in the unit cell, which is energetically not favored. Nevertheless,  $E_{p,(11 \times \sqrt{3})}$  is pretty close to the experimentally predicted value of 1.1 eV by Scoles group.<sup>37</sup> When the chemisorption energies of C10 in the standing up  $(\sqrt{3} \times \sqrt{3})$  and in the lying down  $(11 \times \sqrt{3})$  structures are compared, the latter comes out as being slightly more stable in agreement with the previous theoretical studies.<sup>31</sup> This result indicates that alkyl chain-gold surface interactions are stronger than the chain-chain interactions supporting the discussion made above regarding chain length dependence of  $(\sqrt{3} \times \sqrt{3})$  adsorption energies.

For extrapolating the  $S_c$  and  $S_p$  values (discussed above for lying down isolated molecules) to monolayer coverage in order to have a better comparison with the experimentally reported value, we used the ratio of  $(11 \times \sqrt{3})$  chemisorption energy to that of isolated lying down C10 (calculated with PBE+dDsC). When  $S_c$  and  $S_p$  are divided by this ratio (1.17) the resulting corrected slopes, -0.10 eV/n and -0.085 eV/n, are, however, still larger (in magnitude) than the experimental value (0.063 eV/n). This inconsistency with the experimental slopes and the apparent difference between the chemisorption energies reported here for  $(\sqrt{3} \times \sqrt{3})$  phases and the experimental values reported in the literature (determined by temperature programmed desorption studies, TPD) may have common reasons and deserve further elaboration. Experimentally, desorption energies of full monolayer chemisorbed alkanethiols are determined to be about 1.30 eV and do not change with chain length.<sup>13,37,52,53</sup> Though some higher energy desorption features for long alkanethiols (as high as 1.7 eV for C16) were also reported, these energies were not chain length dependent.<sup>13,37,52–54</sup> However, our results indicate much larger energies and more importantly an increase with the chain length. To resolve this “inconsistency” it should be kept in mind that during TPD measurements the temperature of the film is ramped and desorption takes place gradually. Hence, before desorbing from the surface (before Au-S bond is broken), molecules may detach themselves from the island borders and dif-

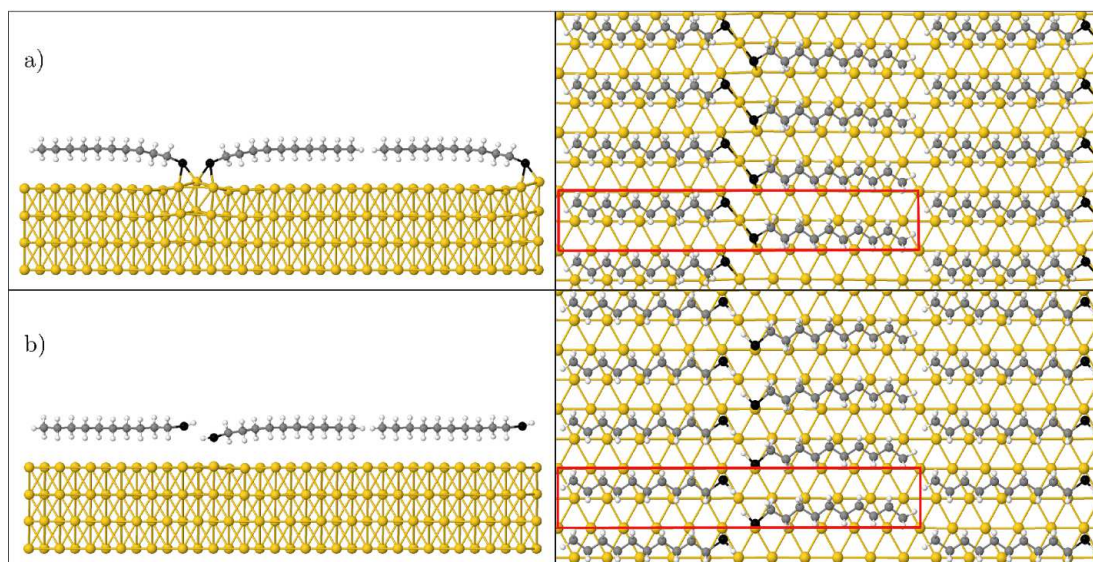


FIG. 10. One full monolayer of decanethiol (C10) on Au(111) with  $(11 \times \sqrt{3})$  structure optimized using the PBE+dDsC vdW corrected DFT functional. Surface unit cell is indicated on the right panel (top view).

fuse on the surface or change their configuration (since the gold potential energy surface is pretty smooth as evidenced by many previous computational studies). Such a detachment from island edges than could eliminate the chain length dependence of the desorption energies for the chemisorbed phases.

#### IV. CONCLUSIONS

The structures and energetics of isolated and monolayer phases of alkanethiols on gold (111) surface have been investigated by density functional theory calculations. In order to put forward the role of dispersive forces on these metal-organic systems, vdW corrections have also been included in the calculations using the density dependent dDsC scheme. In all cases, considered in this study, physisorption of alkanethiols (C1-C10) ends up with the S atom being on top of a surface Au atom. However, chemisorption leads to strong binding at the bridge site with the formation of two almost equivalent Au-S bonds. While, PBE results indicate negligible dependence of the binding energies on chain length, dDsC results show an increase in the binding strength with increasing chain length with almost the same rate for both chemisorption ( $-0.10$  eV/n) and physisorption ( $-0.12$  eV/n). The difference between the chemisorption and

physisorption energies and tilt angles indicate that after a chain length of 6 carbons the molecules become flexible enough to interact with the gold surface even in the chemisorbed configuration (where the molecular geometry is constrained by the S-Au bond). It is interesting to note that this chain length ( $n=6$ ) coincides with the estimated chain length for which the energy of the transition state between chemisorbed and physisorbed states lies below the molecular desorption energy (see Figure 1).

In case of standing up full monolayers the chemisorption energy increases with increasing chain length due to chain-chain interactions with a rate of about ( $-0.1$  eV/n). However, regardless of the chain length chemisorption energy of the full monolayers are always lower (in magnitude) than that of the isolated (lying down) molecules, due to the gold surface stress present in the full monolayer films. The difference between full monolayer and isolated chemisorption energies, however, starts increasing with a rate of  $0.08$  eV/n after  $n = 6$ , indicating that the alkyl chain-gold surface interaction is stronger than chain-chain interactions for alkanethiols with  $n > 6$ . The fact that chemisorption energy for the striped C10 monolayer is slightly larger (in magnitude) than that of the standing up C10 monolayer is also in agreement with this conclusion. In its striped phase C10 lies perfectly parallel to the surface lifting a gold atom up, in agreement with the proposed models for this film in the literature.

\* emete@balikesir.edu.tr

† danisman@metu.edu.tr

<sup>1</sup> Z. Matharu, A. J. Bandodkar, V. Gupta, and B. D. Malhotra, *Chem. Soc. Rev.* **41**, 1363 (2012).

<sup>2</sup> S. A. Claridge, W.-S. Liao, J. C. Thomas, Y. Zhao, H. H. Cao, S. Cheunkar, A. C. Serino, A. M. Andrews, and P. S. Weiss, *Chem. Soc. Rev.* **42**, 2725 (2013).

<sup>3</sup> F. Schreiber, *Progress in Surface Science* **65**, 151 (2000).

- <sup>4</sup> J. C. Love, L. A. Estroff, J. K. Kriebel, R. G. Nuzzo, and G. M. Whitesides, *Chemical Reviews* **105**, 1103 (2005).
- <sup>5</sup> M. D. Porter, T. B. Bright, D. L. Allara, and C. E. D. Chidsey, *Journal of the American Chemical Society* **109**, 3559 (1987).
- <sup>6</sup> C. D. Bain, E. B. Troughton, Y. T. Tao, J. Evall, G. M. Whitesides, and R. G. Nuzzo, *Journal of the American Chemical Society* **111**, 321 (1989).
- <sup>7</sup> C. Vericat, M. E. Vela, G. Corthey, E. Pensa, E. Cortes, M. H. Fonticelli, F. Ibanez, G. E. Benitez, P. Carro, and R. C. Salvarezza, *RSC Adv.* **4**, 27730 (2014).
- <sup>8</sup> P. Maksymovych, O. Voznyy, D. B. Dougherty, D. C. Sorescu, and J. T. Y. Jr., *Progress in Surface Science* **85**, 206 (2010).
- <sup>9</sup> D. P. Woodruff, *Phys. Chem. Chem. Phys.* **10**, 7211 (2008).
- <sup>10</sup> G. E. Poirier, *Langmuir* **15**, 1167 (1999).
- <sup>11</sup> Y. Qian, G. Yang, J. Yu, T. A. Jung, and G.-y. Liu, *Langmuir* **19**, 6056 (2003).
- <sup>12</sup> N. Camillone, T. Y. B. Leung, P. Schwartz, P. Eisenberger, and G. Scoles, *Langmuir* **12**, 2737 (1996).
- <sup>13</sup> E. Albayrak, S. Duman, G. Bracco, and M. Danişman, *Applied Surface Science* **268**, 98 (2013).
- <sup>14</sup> M. Toerker, R. Staub, T. Fritz, T. Schmitz-Hbsch, F. Selam, and K. Leo, *Surface Science* **445**, 100 (2000).
- <sup>15</sup> S. B. Darling, A. W. Rosenbaum, Y. Wang, and S. J. Sibener, *Langmuir* **18**, 7462 (2002).
- <sup>16</sup> H. Kondoh, C. Kodama, H. Sumida, and H. Nozoye, *The Journal of Chemical Physics* **111**, 1175 (1999).
- <sup>17</sup> L. H. Dubois, B. R. Zegarski, and R. G. Nuzzo, *The Journal of Chemical Physics* **98**, 678 (1993).
- <sup>18</sup> T. Shimada, H. Kondoh, I. Nakai, M. Nagasaka, R. Yokota, K. Amemiya, and T. Ohta, *Chemical Physics Letters* **406**, 232 (2005).
- <sup>19</sup> A. Cossaro, R. Mazzarello, R. Rousseau, L. Casalis, A. Verdini, A. Kohlmeier, L. Floreano, S. Scandolo, A. Morgante, M. L. Klein, and G. Scoles, *Science* **321**, 943 (2008).
- <sup>20</sup> Y. Wang, Q. Chi, N. S. Hush, J. R. Reimers, J. Zhang, and J. Ulstrup, *The Journal of Physical Chemistry C* **115**, 10630 (2011).
- <sup>21</sup> H. Kondoh and H. Nozoye, *The Journal of Physical Chemistry B* **103**, 2585 (1999).
- <sup>22</sup> Q. Guo and F. Li, *Phys. Chem. Chem. Phys.* **16**, 19074 (2014).
- <sup>23</sup> L. Tang, F. Li, W. Zhou, and Q. Guo, *Surface Science* **606**, L31 (2012).
- <sup>24</sup> O. Voznyy, J. J. Dubowski, J. T. Yates, and P. Maksymovych, *Journal of the American Chemical Society* **131**, 12989 (2009).
- <sup>25</sup> C. Vericat, M. E. Vela, G. Benitez, P. Carro, and R. C. Salvarezza, *Chem. Soc. Rev.* **39**, 1805 (2010).
- <sup>26</sup> G. S. Longo, S. K. Bhattacharya, and S. Scandolo, *The Journal of Physical Chemistry C* **116**, 14883 (2012).
- <sup>27</sup> M. P. Quiroga Arganaraz, J. M. Ramallo-Lopez, G. Benitez, A. Rubert, E. D. Prieto, L. M. Gassa, R. C. Salvarezza, and M. E. Vela, *Phys. Chem. Chem. Phys.* **17**, 14201 (2015).
- <sup>28</sup> P. Carro, E. Pensa, C. Vericat, and R. C. Salvarezza, *The Journal of Physical Chemistry C* **117**, 2160 (2013).
- <sup>29</sup> R. Nadler, R. S. de Armas, and J. F. Sanz, *Computational and Theoretical Chemistry* **975**, 116 (2011).
- <sup>30</sup> E. Torres, A. T. Blumenau, and P. U. Biedermann, *ChemPhysChem* **12**, 999 (2011).
- <sup>31</sup> L. Ferrighi, Y.-x. Pan, H. Grönbeck, and B. Hammer, *The Journal of Physical Chemistry C* **116**, 7374 (2012).
- <sup>32</sup> D. Otálvaro, T. Veening, and G. Brocks, *The Journal of Physical Chemistry C* **116**, 7826 (2012).
- <sup>33</sup> J. L. C. Fajín, F. Teixeira, J. R. B. Gomes, and M. N. D. S. Cordeiro, *Theoretical Chemistry Accounts* **134**, 67 (2015).
- <sup>34</sup> K. Forster-Tonigold and A. Groß, *Surface Science* **640**, 18 (2015).
- <sup>35</sup> N. B. Luque, E. Santos, J. Andres, and F. Tielens, *Langmuir* **27**, 14514 (2011).
- <sup>36</sup> F. Schreiber, A. Eberhardt, T. Y. B. Leung, P. Schwartz, S. M. Wetterer, D. J. Lavrich, L. Berman, P. Fenter, P. Eisenberger, and G. Scoles, *Phys. Rev. B* **57**, 12476 (1998).
- <sup>37</sup> D. J. Lavrich, S. M. Wetterer, S. L. Bernasek, and G. Scoles, *The Journal of Physical Chemistry B* **102**, 3456 (1998).
- <sup>38</sup> C. Munuera, E. Barrena, and C. Ocal, *Langmuir* **21**, 8270 (2005).
- <sup>39</sup> G. Kresse and J. Hafner, *Phys. Rev. B* **47**, 558 (1993).
- <sup>40</sup> G. Kresse and J. Furthmüller, *Phys. Rev. B* **54**, 11169 (1996).
- <sup>41</sup> P. E. Blöchl, *Phys. Rev. B* **50**, 17953 (1994).
- <sup>42</sup> G. Kresse and D. Joubert, *Phys. Rev. B* **59**, 1758 (1999).
- <sup>43</sup> R. W. G. Wyckhoff, *Crystal Structures*, 2nd ed. (Interscience Publishers, New York, 1958).
- <sup>44</sup> K. Lee, E. D. Murray, L. Kong, B. I. Lundqvist, and D. C. Langreth, *Phys. Rev. B* **82**, 081101 (2010).
- <sup>45</sup> S. N. Steinmann and C. Corminboeuf, *The Journal of Chemical Physics* **134**, 044117 (2011).
- <sup>46</sup> S. N. Steinmann and C. Corminboeuf, *Journal of Chemical Theory and Computation* **7**, 3567 (2011).
- <sup>47</sup> S. Gautier, S. N. Steinmann, C. Michel, P. Fleurat-Lessard, and P. Sautet, *Phys. Chem. Chem. Phys.* **17**, 28921 (2015).
- <sup>48</sup> M. C. Vargas, P. Giannozzi, A. Selloni, and G. Scoles, *The Journal of Physical Chemistry B* **105**, 9509 (2001).
- <sup>49</sup> F. P. Cometto, P. Paredes-Olivera, V. A. Macagno, and E. M. Patrito, *The Journal of Physical Chemistry B* **109**, 21737 (2005).
- <sup>50</sup> P. Lustemberg, P. Abufager, M. Martiarena, and H. Busnengo, *Chemical Physics Letters* **610-611**, 381 (2014).
- <sup>51</sup> R. Mazzarello, A. Cossaro, A. Verdini, R. Rousseau, L. Casalis, M. F. Danisman, L. Floreano, S. Scandolo, A. Morgante, and G. Scoles, *Phys. Rev. Lett.* **98**, 016102 (2007).
- <sup>52</sup> E. Albayrak and M. F. Danişman, *The Journal of Physical Chemistry C* **117**, 9801 (2013).
- <sup>53</sup> E. Albayrak, S. Karabuga, G. Bracco, and M. F. Danişman, *The Journal of Chemical Physics* **142**, 014703 (2015).
- <sup>54</sup> R. G. Nuzzo, L. H. Dubois, and D. L. Allara, *Journal of the American Chemical Society* **112**, 558 (1990).